

A Permanent Magnet Generator for Small Scale Wind Turbines

J. R. Bumby, N. Stannard and R. Martin

Abstract—This paper describes the development of a permanent magnet generator for small scale wind turbines. The generator has been designed for ease of manufacture so that it can be made by small mechanical engineering companies with limited electrical engineering knowledge. The generator has also been designed to have no cogging torque so that it can be used with all horizontal and vertical axis turbine designs. The generator efficiency is very high, particularly at part load. Typical efficiency values are 93-94%.

Index Terms—Wind power; Permanent magnet generators.

I. INTRODUCTION

SMALL SCALE wind turbines (less than 20 kW) are typically designed and manufactured by relatively small mechanical engineering companies. One component that causes particular problems is the electrical generator as suitable generators are not always readily available. In the case of mains-connected turbines the manufacturer is sometimes forced down the route of using a gearbox and standard 4-pole induction machine. For smaller turbines the manufacturer is inevitably looking at a specially built generator such as those described in [1] and [2]. Many of these turbine developers would like to employ a direct drive generator (no gearbox) whilst having a generator design that is mechanically simple, so enabling them to build their own if necessary. The generator must also be mechanically robust, cheap to make and easily integrated into the turbine system. It must also be easily modified for mains-connection operation, battery charge operation or for resistance heating. In addition it should produce no cogging torque to avoid any self-starting issues associated with some types of wind turbine.

One generator that meets all these criteria is an axial-flux air-cored machine with concentrated armature coils [3][4]. In this paper the design of this type of axial-flux generator is described along with its use in two vertical axis wind turbines (VAWT); a 500W Savonius turbine, Figure 1, and a 2.5 kW Darrius type turbine, Figure 2 [5]. The predicted performance

of the generator for mains-connect or battery charge operation are compared with measured data.



Fig. 1. Savonius VAWT (courtesy Rugged Renewables)



Fig. 2. "H" bladed wind turbine (courtesy Carbon Concepts)

II. THEORY

A. Generator topology

The generator consists of two rotor discs mounted either side of a non-magnetic, non-conducting stator, Fig. 3. The magnets are mounted in a N-S-N-S arrangement circumferentially

Manuscript received June 30, 2006.

Jim Bumby is with the School of Engineering, Durham University, South Road, Durham UK. DH1 3LE (Telephone: +44 191 3342404; fax: +44 191 3342408; e-mail: j.r.bumby@durham.ac.uk).

Nick Stannard is with the School of Engineering, Durham University, South Road, Durham UK. DH1 3LE (e-mail: nick.stannard@durham.ac.uk).

Richard Martin is with the School of Engineering, Durham University, South Road, Durham UK. DH1 3LE (e-mail: richard.martin@durham.ac.uk).

round each rotor plate with the N magnet on one plate facing a S magnet on the other. The flux travels directly across the “air” space between the rotor discs before turning circumferentially in the rotor disc and travelling one pole pitch before returning back across the air-gap. A non-magnetic, non-conducting stator holds a number of circular bobbin wound armature coils positioned circumferentially round the stator. Although generators can readily be designed for any number of phases the generators described in this paper are all three phase machines with 16 magnets per disc and 12 armature coils. This combination gives a 240° phase shift between adjacent armature coils and provides for 4 coils per phase. By using simple bobbin wound armature coils it is straightforward to connect the four armature coils per phase in an appropriate series/parallel arrangement so that the generator is suitable for either mains-connect or battery charging. Alternatively, armature coils with a different number of turns can be used, the manufacturer simply selecting the appropriate coils for the application.

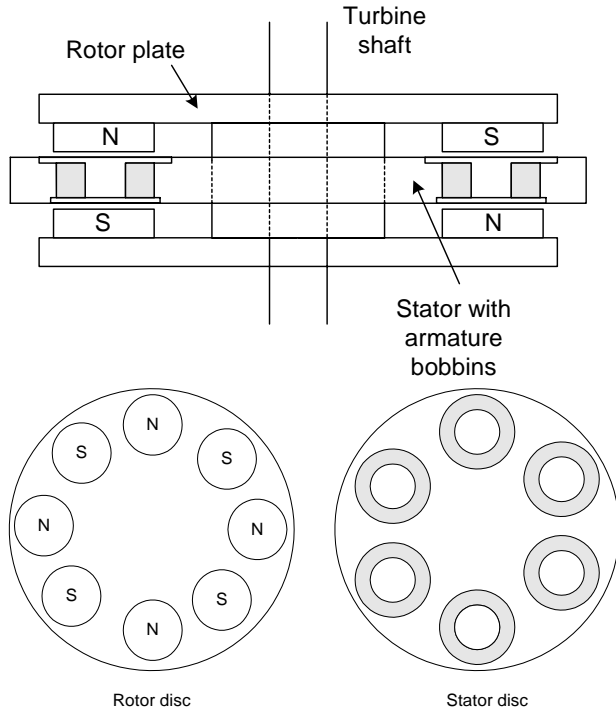


Fig. 3. Generator topology

B. Electrical design equations

The magnetic field distribution from the 16 magnets for the 1 kW generator is shown in Fig. 4. The flux density distribution is approximately sinusoidal in both the radial and circumferential directions so that the flux density profile over a magnet pitch can be thought of as a “sinusoidal hill” described by [3]

$$B_{yn}(x) = \left[\frac{\hat{J}_n \mu_0}{u_n} \frac{\sinh u_n \frac{t_m}{2}}{\sinh u_n \frac{g}{2}} \right] \cos u_n x = \hat{B}_n \cos u_n x \quad (1)$$

where \hat{J}_n is the magnet equivalent current density given by

$$\hat{J}_n = \frac{4}{\tau} \frac{B_{rem}}{\mu_0 \mu_{rec}} \sin \frac{u_n}{2} d_m \quad \text{A/m}^2 \quad (2)$$

and B_{rem} is the magnet remanence, d_m the magnet diameter, τ the pole pitch and $u_n = \frac{\pi m}{\tau}$ [6]. The assumption of the magnetic

flux density forming a “sinusoidal hill” implies an axis-symmetric flux density distribution around each magnet with x being the radial distance from the centre of the magnet. This flux density profile can now be used to derive the flux between the centre of the armature coil and the radius r_a as

$$\phi_a = 2\pi \hat{B}_1 \left[\left(\frac{1}{u_1} \right)^2 (\cos u_1 r_a - 1) + \frac{1}{u_1} (r_a \sin u_1 r_a) \right] \quad (3)$$

If it is assumed that the armature coil is concentrated at its mean axial position, but that the coil is divided into three segments a, b and c in the radial direction, with the turns in each of these segments concentrated at the mean radius of that segment, then the total flux linkage is given by

$$\hat{\lambda} = \frac{N}{3} (\phi_a + \phi_b + k_I \phi_c) \quad (4)$$

and the coil emf by

$$E_{coil} = \frac{2\pi}{\sqrt{2}} f \hat{\lambda} = 4.44 f \hat{\lambda} \quad (5)$$

In equation (4) a flux enhancement factor k_I is introduced ($k_I \geq 1$) to compensate for the fact that the flux calculated in the outer coil segment will be slightly less than actual. This is because the analysis assumes the flux density to be sinusoidally distributed in all directions round the magnet. However, this is only strictly true in the generator circumferential direction and not the radial as in this direction the flux density simply reduces to zero. Thus the flux calculated for the outer coil segment will be a slight underestimate. Typically $k_I = 1.05$ is used to compensate for this.

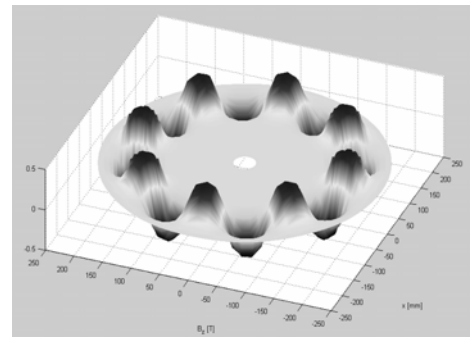


Fig.4. Flux density distribution at the axial centre of a 12/16 generator

A similar approach can be taken in calculating the coil inductance but now the flux profile is assumed to conical with a trapezoidal cross section. The inductance of an armature coil is then given by [3]

$$L_{coil} = k_L \hat{\lambda} \quad (6)$$

with the coil flux linkage given by

$$\lambda = B_a N \pi r_i^2 + 2 \frac{B_a N \pi}{(r_o - r_i)^2} \left(\frac{1}{12} r_o^4 - \frac{1}{2} r_o^2 r_i^2 + \frac{2}{3} r_i^3 r_o - \frac{1}{4} r_i^4 \right) \quad (7)$$

where B_a is the peak coil flux density $B_a = \mu_0 \frac{N}{g}$, r_i and r_o are the coil inner and outer radii respectively, and k_L is a flux leakage factor. Full details of this analysis can be found in [3].

C. Performance equations

The three phase generator output can be dissipated in a three phase resistor bank or, more usually, the output is rectified and used either to charge batteries or used directly as the dc link voltage to supply a grid tie inverter such as the SMA Windy Boy[7] as shown in Fig. 5.

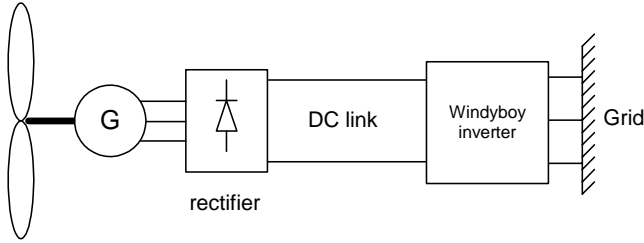


Fig. 5. Connection of Windy Boy to mains

In either case the generator and rectifier are conveniently represented by an equivalent circuit viewed from the dc side of the rectifier. Such an equivalent circuit is shown in Fig. 6 for battery charge applications. The battery is simply represented by its internal resistance and open circuit emf whilst the generator is modeled by its open circuit emf, its equivalent resistance and the equivalent overlap resistance [8]. If required an additional voltage is easily included to represent the diode volt drop in the rectifier.

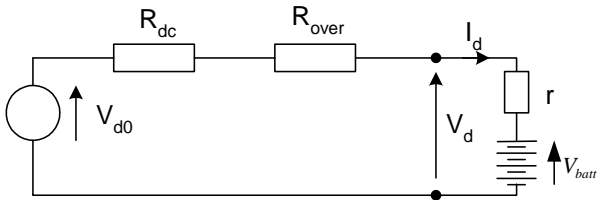


Fig. 6. Equivalent dc circuit for battery charging.

For a three-phase, 6-pulse, rectifier the effective armature resistance is approximately twice the phase resistance i.e.

$$R_{dc} \approx 2R_{ph} \quad (8)$$

The overlap resistance is given by

$$R_{over} = \frac{3}{\pi} \omega L_{ph} \quad (9)$$

and the open circuit emf is related to the phase voltage by

$$V_{d0} = \frac{3\sqrt{2}}{\pi} E_{line} = 2.34 E_{ph} \quad (10)$$

Simple circuit analysis gives the current as

$$I_d = \frac{V_{d0} - V_{batt}}{R_{dc} + R_{over} + r} \quad (11)$$

And the battery terminal voltage as

$$V_d = V_{d0} - I_d R_{dc} - I_d R_{over} \quad (12)$$

The power supplied to the battery is now readily calculated as

$$P_{batt} = V_d I_d \quad (13)$$

For mains connect applications through the grid-tie inverter the battery is simply replaced by the dc link capacitance and

the mains connect inverter is modeled by its power transfer characteristics, Fig. 7. In the case of the SMA Windy Boy the power transfer characteristic is a linear function that depends on the dc link voltage [7]. As the generator used is a PM generator, then, to a first approximation, the power transfer is a direct function of turbine speed (neglecting voltage drops in the armature resistance and overlap resistance).

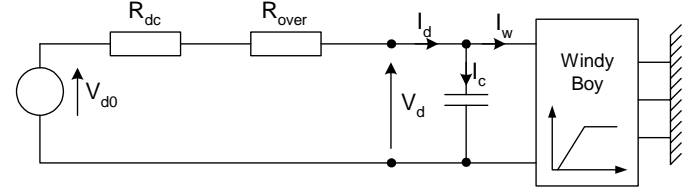


Fig. 7 Windy Boy equivalent circuit

For the Windy Boy to operate there must be a dc voltage of at least 260V. The dc link voltage that will correspond to maximum power transfer can be set at any voltage up to 600V. If set at, say, 450V then the inverter would transfer power as a linear function of voltage between 260 and 450V and above 450V would keep the power constant until the over-voltage cut-off condition is reached. This must be below 600V. The analysis is similar to before except now the power transfer through the inverter determines the current I_w as

$$I_w = \frac{P_w}{V_d} \quad (14)$$

With the remaining equations being

$$I_d = \frac{V_{d0} - V_d}{R_{dc} + R_{over}} \quad (15)$$

$$I_c = I_d - I_w \quad (16)$$

$$V_c = \frac{1}{C} \int I_c dt \quad (17)$$

If feeding a resistive load the generator is simply represented by its per phase equivalent circuit shown in Fig. 8. Analysis of this circuit is straight-forward and gives the terminal power per phase as

$$P = \frac{E^2}{(R_{ph} + R_L)^2 + X_{ph}^2} R_L = \frac{k^2 \omega^2}{(R_{ph} + R_L)^2 + X_{ph}^2} R_L \approx \frac{k^2 \omega^2}{R_L} \quad (18)$$

where k is the machine constant and ω the rotational speed in rad/s. Provided the load resistance is significantly greater than the generator resistance and reactance (normal), then the final approximation relating power output to generator speed and load resistance holds.

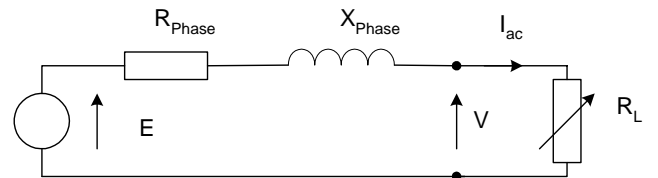


Fig. 8. A.C. equivalent circuit for a resistive load.

III. EXPERIMENTAL MACHINES

Two experimental machines have been constructed: a 1kW generator for a Savonius wind turbine and a 2.5 kW generator for the "H" bladed turbine. Although the original specification for the Savonius turbine was for a 1 kW generator the final turbine built was a 500W machine so that the generator is

over-rated for the application. Nevertheless, the generator has operated successfully on this turbine for a period of about 2 years. This 1kW, 300 rpm generator is also ideally suited to a 2kW, 500 rpm water turbine application.

The basic mechanical design of both generators is similar and both have 16 magnets per rotor disc and 12 armature coils. Both are three-phase generators. The main difference between the two designs is the way in which they have been designed to integrate mechanically with their respective turbines. Both can be regarded as “bearingless” designs as the bearings in both are also the turbine bearings.

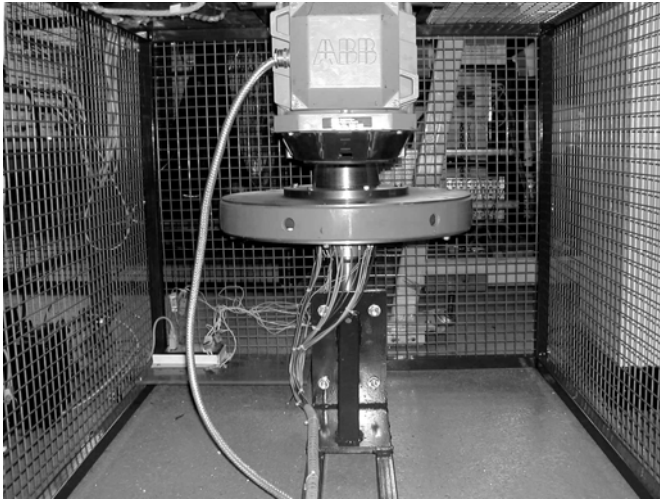


Fig. 9. 1kW generator on test in the laboratory.



Fig.10. The 2.5 kW generator (Mark 1 version)

The 1kW version is shown on test in the laboratory in Fig. 9. The shaft system consists of inner and outer concentric shafts to allow the Savonius turbine to be bolted onto a top flange. In contrast, the 2.5kW generator is built round a central hub with one of the rotor discs also being used to support the turbine blades. This generator is shown in Fig. 10. The stator and one of the rotor discs of the 1kW generator are shown in Fig. 11. Clearly visible in this picture are the armature bobbin-coils located in a non-magnetic, non-conducting stator, in this case PVC. The 16 magnets on one rotor disc are seen located on the rotor by a PVC location ring. A summary of the two generator designs is given in Table 1.

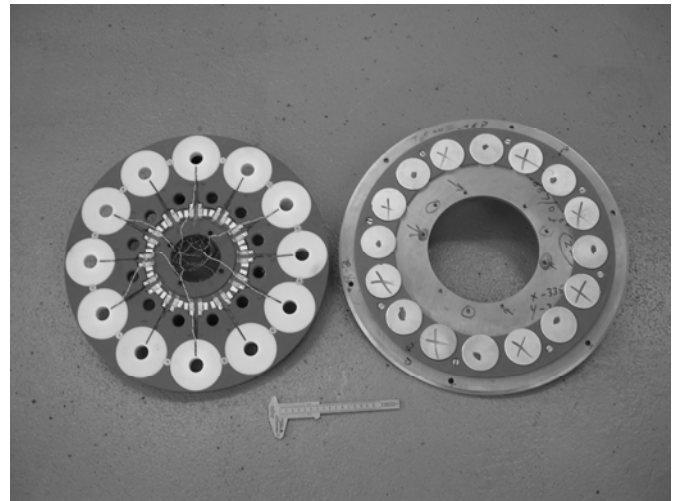


Fig. 11. Stator and rotor discs of the 1 kW generator.

		1kW	2.5kW
Rated power	W	1000	2500
Rated speed	rpm	300	250
Rated frequency	Hz	40	33.3
Rated EMF (per coil)	V	33.6	205
Number of phases		3	3
Number of pole pairs		8	8
Number of armature coils		12	12
Generator diameter	mm	462	590
Generator length	mm	55	60

Table 1. Generator data

IV. RESULTS

A. Generator Parameters

A comparison of measured and predicted generator parameters is given in Table 2. Predicted values are in general very good with differences between measured and predicted being within 5%.

	1 kW		2.5 kW	
	Measured	Predicted	Measured	Predicted
Coil inductance (mH)	4.67	4.59	67	81
Coil resistance (ohms)	1.02	0.97	12.9	11.1
V/100rpm/coil	11.03	11.2	86.0	82.1

Table 2. Generator Parameters

B. 1 kW Savonius generator

The parameter values in Table 2 can be used along with the performance equations in section II to predict generator performance and compare this with measured data. However, it is also important to match the generator design to the turbine performance. For the Savonius turbine the expected power curves at wind speeds between 6 and 15 m/s are shown in Fig. 12. Also shown on this figure are the measured and predicted load curves with the generator operating into a three-phase resistive load. In these test all four of the generator coils per phase were connected in series to give a generator open-circuit of 44V/100rpm. The loading curves are essentially parabolic as the generator power loading is proportional to speed² and inversely proportional to resistance, as explained

in equation (18). As the loading is increased (resistance decreased) the loading curves become progressively steeper such that a resistive load of about 122 ohms per phase gives an ideal turbine loading. Such resistive load tests are ideal when trying to evaluate actual turbine performance.

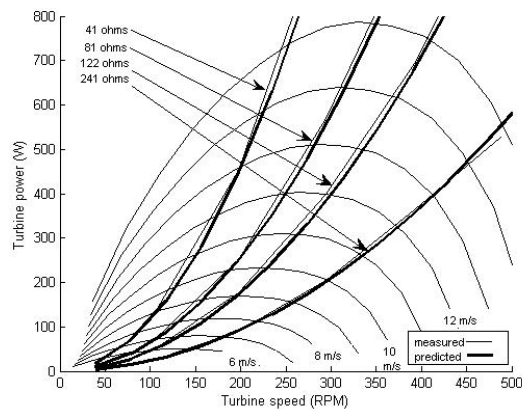


Fig. 12. Resistive load curves for the Savonius turbine

When used for charging a 48V battery, the performance of the generator is shown in Fig. 13. In this case the battery voltage essentially sets the dc voltage and hence the generator speed. Some speed variation occurs due to the voltage drop in the resistive components.

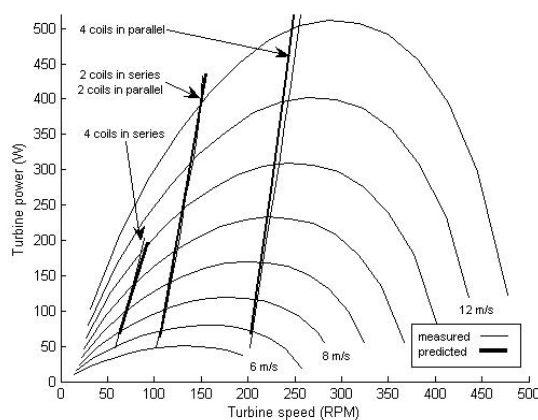


Fig. 13. Battery charging performance

The graph in Fig. 13 demonstrates that for this application a low voltage winding is required and that connecting all the coils in parallel is beneficial. However, with all the coils in parallel the turbine must turn at about 200 rpm before it would produce sufficient voltage to turn the rectifiers on. At speeds below this the battery voltage is greater than the generator voltage and no current will flow. The consequence of this is that at low wind speeds there would be no battery charging and as wind speed increases the turbine is not optimally loaded. At these low wind speeds it would be beneficial to operate with two of the armature coils in series and two in parallel switching over to all four in parallel at wind speeds above about 6 m/s. Again, predicted and measured data are very similar.

When operating through a Windy Boy inverter it is necessary to connect all the coils in series. The measured and predicted power transfer is shown in Fig. 14. In this test the

generator was operated at speeds of up to 500 rpm when power transfers of 2kW were achieved.

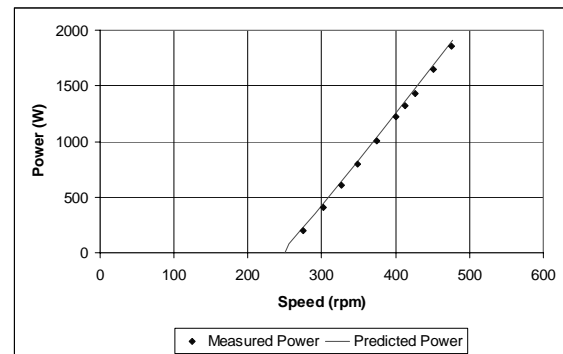


Fig. 14. Windy Boy load characteristic

As the Savonius wind turbine is only rated at 500W the low power end of this characteristic can be superimposed on the turbine power curve as shown in Fig. 15. At low wind speeds the loading is less than ideal (optimal line). If the number of turns on each of the armature coils is increased to 828, by using a lighter gauge wire, then the inverter load curve is easily matched to the turbine characteristics – but note that the armature resistance and inductance would also change. The result of this coil change is shown by the dotted curve in Fig. 15. Such a change is easily made in the generator design due to the modular nature of the design and the use of bobbin wound coils, see Fig. 11.

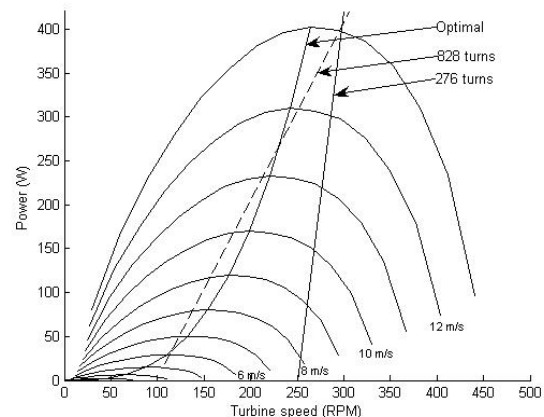


Fig. 15. Windy Boy load characteristic showing Savonius power curves.

B. 2.5kW Generator

This generator has been extensively tested to measure its efficiency when operating into a resistive load and when transferring power through a 2.5 kW Windy Boy grid-tie inverter. Input torque was measured using a torque transducer and output power using a power analyzer. The efficiency of the generator operating into a resistive load is shown in Fig. 16 and when operating through the grid-tie inverter in Fig. 17. In both cases the efficiency includes the effect of bearing loss and generator windage but the dominant loss mechanism is armature Joule loss.

When operating into a resistive load, Fig. 16, the part load efficiency peaks at 96% and drops to about 90% when the current is substantially above rated. For example, at the rated

speed of 250 rpm and powers between 750 and 1500 W, the efficiency is 96% reducing to 93% at rated power of 2.5 kW. As power is further increased above rated power to a value of 3kW, the efficiency reduces to 90%. The thermal rating of the coils will accept power outputs well in excess of 3kW at 250 rpm but at a reduced generator efficiency.

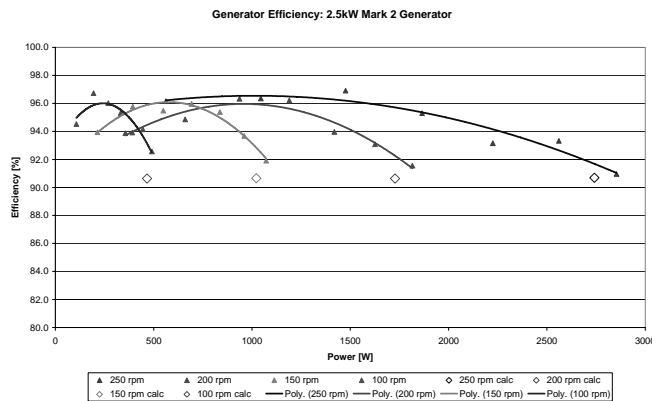


Fig. 16. Measured and predicted efficiency of the 2.5 kW generator operating into a resistive load.

When the generator output is rectified and connected to the mains through an inverter, the efficiency is consistently above 90% and reaches a maximum efficiency of 95%, Fig. 17. When the 2.5 kW power rating of the inverter is reached the power output remains constant but the increase in speed and dc link voltage means that the generator current reduces and the efficiency increases back towards 95%.

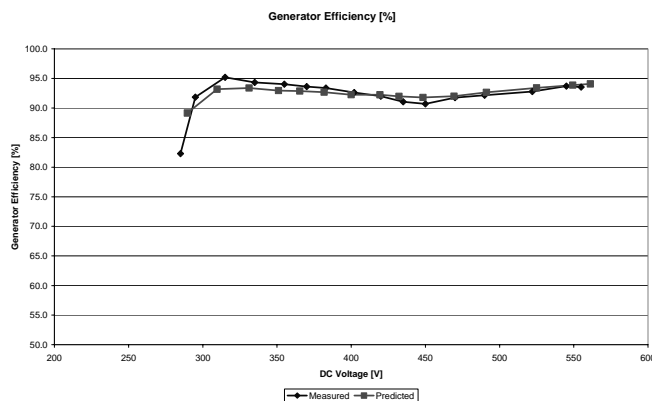


Fig. 17. Measured and predicted efficiency of the 2.5 kW generator operating through a Windy Boy inverter.

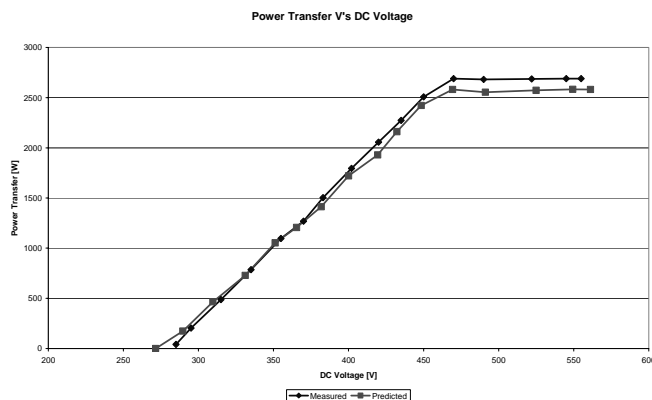


Fig. 18. Measured and predicted power transfer of the 2.5 kW generator operating through a Windy Boy inverter.

The predicted power transfer through the inverter is compared with that measured in Fig. 18. Again excellent agreement is obtained further giving confidence in the analysis and design procedure.

V. CONCLUSION

This paper had described the design, manufacture and performance of a permanent magnet generator for use with small scale wind turbine. The generator is also ideally suitable for use with small water turbines. It is also easy to manufacture and with materials easily separated for reclamation at the end of its life. The generator produces no cogging torque and has an efficiency of typically 93-94%. Part load efficiency is particularly good. The modular winding design allows different coil arrangements and armature voltages to be readily accommodated. Predicted and measured performance, both at ac, and when operating through a rectifier, are in excellent agreement, with a maximum difference of 5%.

ACKNOWLEDGMENT

The work of Alex Wong in designing and building the experimental generator and test rig for the Savonius wind turbine is also gratefully acknowledged. The help and advice given by Peter Reed and Ken England of Rugged Renewables and John Dominy and Nick McCloud of Carbon Concepts is also gratefully acknowledged.

REFERENCES

- [1] Polinder, H.; "Design of a PM generator for the Turby, a wind turbine generator for the built environment", 16th International Conference on Electrical Machines, Cracow, Poland, 5-8th September 2004, paper OS13-6.
- [2] Chalmers, B.J., Wu, W. and Spooner, E., "An axial flux permanent magnet generator for a gearless wind energy system", IEEE Trans. On Energy Conversion, Vol. 14, No. 3, June 1999, pp 749-753
- [3] Bumby, J.R. and Martin, R. "Axial-flux permanent-magnet air-cored generator for small-scale wind turbines", Proc. IEE – Electrical Power Applications, Vol. 152, No. 5, September 2005, pp 1065-1075
- [4] Bumby, J.R. British Patent Application No 0412085.3 "Axial-flux, Permanent Magnet Electrical Machine", 29 May, 2004
- [5] Carbon Concepts, Vertical axis-wind turbine and generator, <http://www.carbonconcepts.co.uk/>, 29 June, 2006
- [6] Bumby, J.R., Martin, R., Spooner, E., Brown, N.L. and Chalmers, B.J. "Electromagnetic design of axial flux permanent magnet machines", Proc. IEE – Electrical Power Applications, Vol. 151, No. 2, March 2004, pp 151-160
- [7] Windy Boy Grid Connect Inverter, <http://www.sma-america.com/windyboy.html#2500>, November 30th, 2004
- [8] Mohan, N., Underland, T.M. and Robbins W.P "Power Electronics – Converters, Applications and Design", John Wiley and Sons, Third Edition, 2003, ISBN 0-471-429078-2.